



Research Article

Enhancing power system stability through intelligent STATCOM control strategies in torsional oscillation environments

Sangeeta BAMBA^{1,*}, Sushil Kumar GUPTA¹

¹Department of Electrical Engineering, Deenbandhu Chhoturam University of Science and Technology, Sonapat, Haryana, 131039 India

ARTICLE INFO

Article history

Received: 11 March 2024

Revised: 15 April 2024

Accepted: 26 May 2024

Keywords:

Grey Wolf Optimization (GWO); Proportional-Integral Controller; Static Synchronous Compensator (STATCOM); Sub Synchronous Resonance (SSR)

ABSTRACT

This research develops a new control method for the IEEE Second benchmark model (SBM) that uses an intelligent optimization-based static synchronous compensator to reduce low-frequency torsional oscillations. This low-frequency oscillation caused by mainly shunt and series compensation produces torsional oscillation and induction generator effect in a synchronous generator that may lead to fatigue in the shaft and continuation of low-frequency oscillations for a long duration. To minimize this effect, various techniques have been applied. The Static Synchronous Compensator's gate signal is managed by the control strategy using two distinct proportional-integral (PI) controllers in accordance with system voltage. The test system is subjected to a three-phase LLL-G fault with zero inherent dampening considered to simulate the most severe situation, with natural damping for comparative analysis. The time-domain outcomes of the rotor dynamics for different test scenarios with and without the Static Synchronous Compensator and with the proposed PSO (Particle swarm optimization), FF (Firefly algorithm), and GWO (Grey Wolf Optimizer) Optimization-based Static Synchronous Compensator (STATCOM). The efficiency of the proposed controller in reducing overall power system oscillations is demonstrated using optimization-based STATCOM. The proposed study demonstrates the superiority of the GWO optimization technique over FF, PSO, and standard STATCOM in terms of settling time. This is evidenced by comparing the simulation results, including the performance index.

Cite this article as: Bamba S, Gupta SK. Enhancing power system stability through intelligent STATCOM control strategies in torsional oscillation environments. Sigma J Eng Nat Sci 2024;42(6):1933–1953.

INTRODUCTION

Power system stability refers to the capacity of the system to maintain its steady operational condition in the presence of disturbances[1]. These disturbances can vary in magnitude, ranging from significant to minor. Power

systems often face the significant problem of transient stability when they experience massive disruptions for a short period of time. This results in a need for coordination among the generators in distinct interconnected segments of the system. Significant disruptions can encompass

*Corresponding author.

*E-mail address: 20001902005sangeetabamba@dcrustm.org

This paper was recommended for publication in revised form by Editor-in-Chief Ahmet Selim Dalkılıç



abrupt line loss, faults, or generator failure [2]. The often observed methods for improving transient stability in power systems involve the utilization of an automated voltage regulator (AVR) for excitation control and a speed governor equipped with a steam valve for speed control. In the case of constant steam turbine mechanical power, the excitation system controls the alternators internal voltage. Assuming a constant internally generated voltage, the speed governor uses steam valve control to control the alternators speed. The paper [3-5] discusses the application of linear controllers in AVR and speed governor systems to enhance power system transient stability. Linear approach controllers are the most effective tools when it comes to tackling challenges that are related to dynamic stability.

Non-linear controllers are mainly used to address transient stability. Using a synchronous motor-generator pair, the power system's stability was improved in a study that employed a lot of renewable energy [6]. With the use of a distributed power controller, multi-machine power systems can achieve transient stability augmentation, as mentioned in [7]. The improvement of power system stability through the mitigation and regulation of subsynchronous resonance (SSR) utilizing a large-scale photovoltaic (PV) plant has been examined in previous studies [8,9]. A comprehensive photovoltaic (PV) system is managed in order to mitigate power system oscillations, as demonstrated in [10]. According to [11-13] a thyristor-controlled series capacitor (TCSC) controller has been designed using modal control in order to reduce torsional oscillations in a power system.

The recent advancement in the electrical and electronic power sectors has increased FACTS utilization in electric power systems for various control objectives. Implementing FACTS devices in power systems results in numerous benefits, such as decreased operational expenses, improved system dependability and security, and an expansion of the transfer ability of existing transmission lanes within the deregulated electricity sector. The research paper [14] comprehensively explains various FACT controllers and their specific applications. With FACT controllers, low-frequency power oscillations can be lessened, and the system's voltage profile can be maintained by efficiently controlling the flow of real and reactive power. In recent times, several FACT controllers like UPFC (Unified power flow controller), SVC (static VAR compensator), and TCSC (thyristor-controlled series capacitor) [13–15] have been utilized in practical power systems. The STATCOM, also known as the static synchronous compensator, is a shunt controller belonging to the FACTS family. It is designed to exchange active power with the system in a transient manner and has superior damping characteristics. Its primary purpose is to enhance the systems dynamic and transient stability, particularly when compared to other counterparts such as the SVC. The paper [15] discusses the STATCOM controller's damping properties in relation to the lead-lag compensator.

Recently, several soft computing techniques such as ABC (Artificial Bee Colony), PSO (particle swarm optimization), (FA) Firefly algorithm, (BWO) Black Widow Optimization, BFOA (Bacteria foraging optimization algorithm), and other hybrid optimization techniques have been developed to improve the stability of power systems by optimizing the tuning and placement of FACT controllers. A local damping controller based on fuzzy logic has been presented for the Thyristor-Controlled Series Capacitor (TCSC) to enhance the transient stability of the power system [16]. It has been addressed and contrasted in [17] that the performance of two modified optimization techniques— ABC and PSO —when combined with the Hybrid Genetic algorithm (H-GA). The paper [18] discusses the utilization of a hybrid method that combines Particle Swarm Optimization (PSO) and Gravitational Search method (GSA) to determine the best configuration of Flexible AC Transmission System (FACT) controllers for enhancing voltage stability. [19] presents a controller design for STATCOM that utilizes honey bee mating optimization (HBMO) to improve the stability of power systems. An enhanced Particle Swarm Optimization (PSO) method was proposed in reference [20] to mitigate and regulate sub-synchronous resonance in wind farms with series compensated Doubly Fed Induction Generator (DFIG) systems. In a recent research paper [21], the effectiveness of a Grey Wolf Optimizer (GWO) - based optimum controller in dampening sub-synchronous resonance in a series-compensated power system network was investigated.

Following reference [21], Table 1 provides a comparative analysis between the proposed work and the existing cutting-edge research.

In conclusion, the integration of soft computing techniques with Flexible AC Transmission System (FACTS) devices presents a comprehensive approach to enhancing the performance and reliability of power systems. By leveraging adaptive control strategies, these technologies offer a range of potential benefits, including improved stability, enhanced voltage regulation, increased power transfer capability, reduced power losses, fast response to dynamic changes, enhanced grid resilience, and optimized asset utilization. Overall, the synergy between soft computing and FACTS devices contributes to a more efficient, reliable, and resilient power infrastructure, ultimately benefiting both utilities and consumers.

By evaluating the possible advantages of fact controllers and optimization strategies based on soft computing. This paper proposes the use of soft computing meta-heuristic algorithms to control a Voltage Source Converter (VSC)-based STATCOM in order to reduce sub-synchronous oscillations and voltage fluctuations in a power system. A unique control strategy is used in STATCOM to manage the gate signal by independently controlling the Alternating and Direct currents. This necessitates the use of two separate PI (proportional-integral) controllers.

Table 1. Comparative analysis between the prior research and the proposed work

Previous Study [Reference]; Year	Controller gain selection		Stability analysis	
	Conventional	Intelligent	Rotor angle	Torsional Mode
[8];2017	-	✓	-	✓
[9], [16];2017	✓	-	-	✓
[16];2017	-	-	✓	-
[10];2019	✓	-	✓	-
[20];2019	-	✓	-	✓
[22];2020	-	✓	✓	-
[23]2021	✓	-	✓	✓
[24];2023	✓	-	-	-
Proposed Study	-	✓	✓	✓

These PI controllers' gain parameters have been adjusted by optimization approaches with PSO, FF, and GWO. The IEEE second benchmark model was employed in the investigation to simulate the SSR study in the MATLAB environment.

MAJOR CONTRIBUTIONS

- In this study, a novel control strategy is devised to dampen the Torsional oscillations in the case of a non-linear system.
- A unique control strategy is presented to manage the STATCOM gate signal. Two distinct PI controllers are used in this technique, which independently control AC and DC currents.
- Utilizing Meta-heuristic optimization techniques inspired by nature, such as firefly, PSO, and GWO, have been applied to optimize the PI controllers' gain parameters.
- The system's stability is investigated by means of time-domain simulations analysis and performance indices derived from different error criteria.
- Comparing the suggested GWO optimization methodology's outcomes to those of the PSO and Firefly serves as additional evidence of its effectiveness.

The subsequent segments of the manuscript are structured as follows: Section 2 details the system configuration, while Section 3 delves into the modeling of STATCOM and its associated control structure. Section 4 elaborates on the optimal adjustment of the controller, employing PSO, GWO, and FF. Results and discussions are exhibited in Section 5, and the manuscript concludes in Section 6 with a justified reference-based conclusion.

System Modeling

To investigate the Sub-synchronous Resonance (SSR) problem, the Study employs a modified IEEE second benchmark model. The system described is a basic configuration consisting of a single machine associated with

an infinite bus [25,26]. The transmission line is equipped with a series compensation, as shown in Figure 1. The compensation considered for this specific case is 55%. In the modeled system, an uncompensated transmission line experiences a three-phase to-ground fault at 0.0222 sec for a duration of 0.0169 sec. A fault catalyzes the amplification of the system's oscillations

A transmission network is connected to the generating unit via a step-up transformer. Low-pressure turbine (LPT) and High-pressure turbine (HPT) are the two turbine units that comprise the mechanical mass system. Additionally, the system includes an exciter and a generator. The magnification of torque in these masses poses a significant risk and can result in substantial damage. The results also demonstrate oscillations in torque and speed.

In order to mitigate Sub synchronous Resonance (SSR) in the system, a Static Synchronous Compensator (STATCOM) has been implemented, as depicted in Figure 1. The STATCOM is linked to the drive system by a coupling transformer. The system data is also chosen based on the design considerations outlined in this study [27]. In the case of a multi-bus system, the optimal location for placement of fact devices has been explained in the reference [28]; however, in this case, the system is of two bus system considered. Therefore, STATCOM is connected to the generator terminal so that feedback signal from the generator can be utilized in the STATCOM.

Mathematical Modeling

The linearized mathematical equations are employed to represent numerous subsystems of the system in order to construct a comprehensive mathematical model. This model can be used for conducting eigenvalue analysis for SSR.

Steam governor-turbine system

The governor-turbine concept is represented by transfer functions, as depicted in Figure 2. The model consists

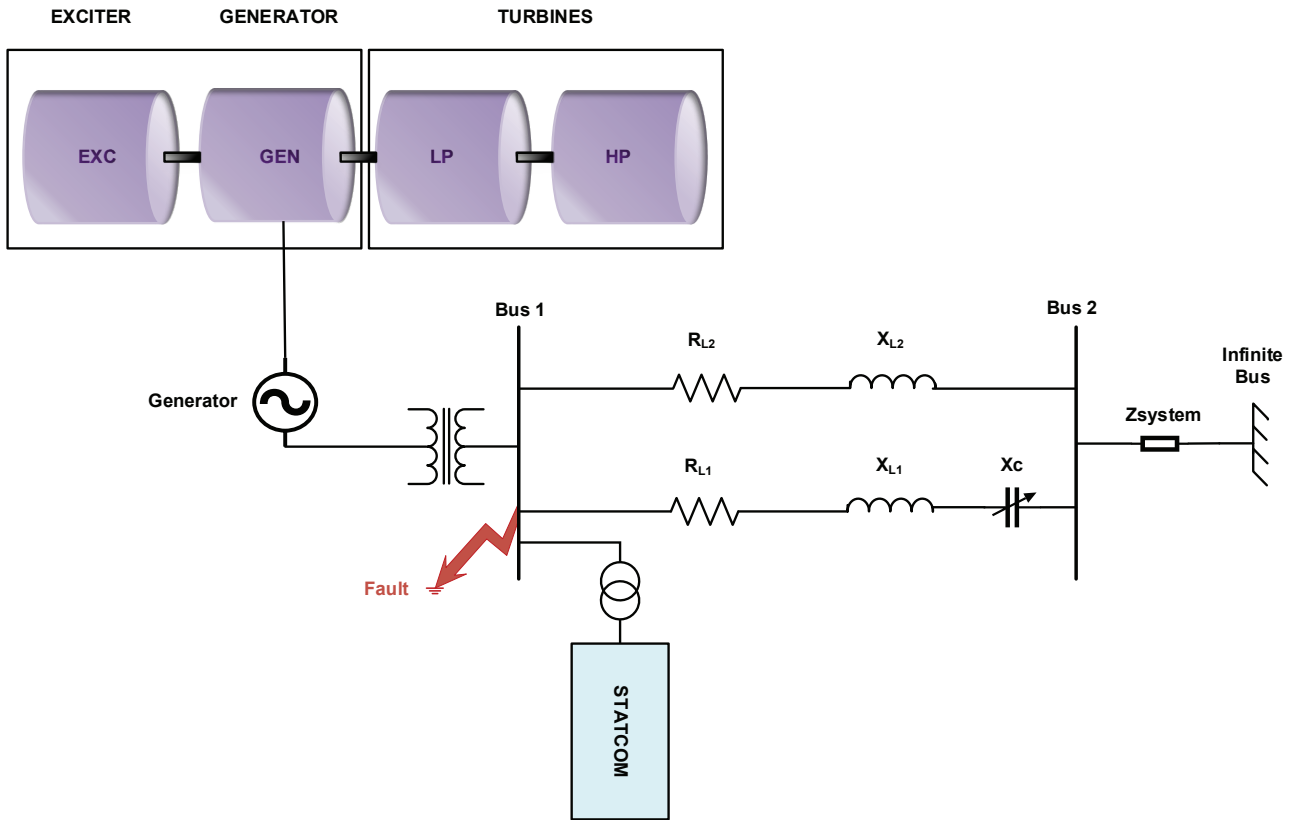


Figure 1. Modified IEEE SBM Model.

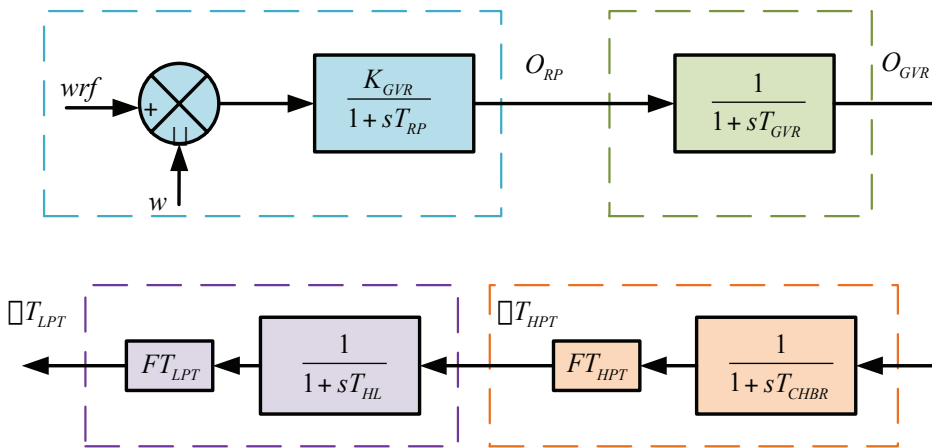


Figure 2. Steam governor-turbine system transfer function model.

of four different temporal constants, namely TRP, TGVR, THL, and TCHBR. The governor is characterized by two distinct temporal constants, TRP and TGVR. The temporal constants associated with steam flow are THL and TCHBR. Torques are directly proportional to each other and contribute to a fraction of the overall torque. The structure of a system can be represented by the equations that follow:

$$\frac{d}{dt} \Delta O_{RP} = \frac{1}{T_{RP}} [k_{GVR} \Delta \omega - \Delta O_{RP}] \tag{1}$$

$$\frac{d}{dt} \Delta O_{GVR} = \frac{1}{T_{GVR}} [\Delta O_{RP} - \Delta O_{GVR}] \tag{2}$$

$$\frac{d}{dt} \Delta \tau_{HPT} = \frac{1}{T_{CHBR}} [F \tau_{HPT} \Delta O_{GVR} - \Delta \tau_{HPT}] \tag{3}$$

$$\frac{d}{dt} \Delta \tau_{LPT} = \frac{1}{T_{HL}} \left[\frac{F \tau_{LPT}}{F \tau_{HPT}} \Delta \tau_{HPT} - \Delta \tau_{LPT} \right] \quad (4)$$

The spring-mass system

Four masses make up the modeled mechanical mass system: the high-pressure turbine (HPT), the low-pressure turbine (LPT), the excitation (X), and the generator (G). Linearized equations express their representation.

High-pressure turbine equations

$$\frac{d}{dt} \Delta \omega_{HPT} = \frac{1}{2H_{HPT}} [-K_{LH} (\Delta \delta_{HPT} - \Delta \delta_{LPT}) - D_{HPT} \Delta \omega + \Delta \tau_{HPT}] \quad (5)$$

$$\frac{d}{dt} \Delta \delta_{HPT} = \omega_0 \Delta \omega_{HPT} \quad (6)$$

Low-pressure turbine equations

$$\frac{d}{dt} \Delta \omega_{LPT} = \frac{1}{2H_{LPT}} [2HX [-D_{LPT} \Delta \omega + \Delta \tau_{LPT} + K_{LH} (\Delta \delta_{HPT} - \Delta \delta_{LPT}) - K_{LG} (\Delta \delta_{HPT} - \Delta \delta_{LPT}) - K_{LG} (\Delta \delta_{LPT} - \Delta \delta_G)] \quad (7)$$

$$\frac{d}{dt} \Delta \delta_{LPT} = \omega_0 \Delta \omega_{LPT} \quad (8)$$

Generator rotor equations

$$\frac{d}{dt} \Delta \omega_G = \frac{1}{2H_G} [-D_G \Delta \omega - \Delta \tau_G + K_{LG} (\Delta \delta_{LPT} - \Delta \delta_G) - K_{GX} (\Delta \delta_G - \Delta \delta_X)] \quad (9)$$

$$\frac{d}{dt} \Delta \delta_G = \omega_0 \Delta \omega_G \quad (10)$$

Excitation system equations

$$\frac{d}{dt} \Delta \omega_X = \frac{1}{2HX} [K_{GX} (\Delta \delta_G - \Delta \delta_X) - D_X \Delta \omega - \Delta \tau_X] \quad (11)$$

$$\frac{d}{dt} \Delta \delta_X = \omega_0 \Delta \omega_X \quad (12)$$

Transmission line

The transmission line is depicted in Figure 1 as a single-line diagram. The linearized form of the presentation is demonstrated in Equations (13-16).

$$X_C \Delta i_{dx} = \frac{1}{\omega_0} \frac{d}{dt} \Delta V_{dcp} - \Delta V_{qcp} \quad (13)$$

$$X_C \Delta i_{qx} = \frac{1}{\omega_0} \frac{d}{dt} \Delta V_{qcp} - \Delta V_{dcp} \quad (14)$$

$$\Delta V_{der} = \frac{X_L}{\omega_0} \frac{d}{dt} \Delta i_{dx} + R_L \Delta i_{dx} - X_L \Delta i_{qx} + \Delta V_{dcp} + V_{diff} \cos(\delta_0) \Delta \delta \quad (15)$$

$$\Delta V_{qter} = \frac{X_L}{\omega_0} \frac{d}{dt} \Delta i_{qx} + R_L \Delta i_{qx} + X_L \Delta i_{dx} + \Delta V_{qcp} + V_{diff} \sin(\delta_0) \Delta \delta \quad (16)$$

Synchronous generator

The generator's linearized equations are derived using Park's voltage equations for synchronous machines in Kundur [2]. The entire system can be readily represented using the aforementioned mathematical formulae. The system's eigenvalue analysis can be performed using a mathematical model.

$$-x_{dx} \frac{d}{dt} \Delta i_{dx} + x_{mdx} \frac{d}{dt} \Delta i_{fd} + x_{mdx} \frac{d}{dt} \Delta i_{Dw} = \omega_0 [(-x_{qx} \Delta i_{qx} + x_{mqx} \Delta i_{Qw} + x_{mqx} \Delta i_{sw}) + \Psi_{q0} \Delta \omega + r_{aw} \Delta i_{dx} + v_{dx}] \quad (17)$$

$$-x_{qx} \frac{d}{dt} \Delta i_{qx} + x_{mqx} \frac{d}{dt} \Delta i_{Qw} + x_{mqx} \frac{d}{dt} \Delta i_{sw} = \omega_0 [(-x_{dx} \Delta i_{dx} + x_{mdx} \Delta i_{fd} + x_{mdx} \Delta i_{Dw} + \Psi_{d0} \Delta \omega + r_{aw} \Delta i_{qx} + v_{qx})] \quad (18)$$

$$-x_{mdx} \frac{d}{dt} \Delta i_{dx} + x_{fd} \frac{d}{dt} \Delta i_{fd} + x_{mdx} \frac{d}{dt} \Delta i_{Dw} = \omega_0 [-r_{fd} \Delta i_{fd} + \Delta v_{fd}] \quad (19)$$

$$-x_{mdx} \frac{d}{dt} \Delta i_{dx} + x_{mdx} \frac{d}{dt} \Delta i_{fd} + x_{Dw} \frac{d}{dt} \Delta i_{Dw} = \omega_0 [-r_{Dw} \Delta i_{Dw}] \quad (20)$$

$$-x_{mqx} \frac{d}{dt} \Delta i_{qx} + x_{Qw} \frac{d}{dt} \Delta i_{Qw} + x_{mqx} \frac{d}{dt} \Delta i_{sw} = \omega_0 [-r_{Qw} \Delta i_{Qw}] \quad (21)$$

$$-x_{mqx} \frac{d}{dt} \Delta i_{qx} + x_{mqx} \frac{d}{dt} \Delta i_{Qw} + x_{sw} \frac{d}{dt} \Delta i_{sw} = \omega_0 [-r_{sw} \Delta i_{sw}] \quad (22)$$

MODELING OF STATCOM AND ITS CONTROL SCHEME: PROPOSED

STATCOM, which belongs to the family of FACT controllers of the shunt type, is highly versatile in its ability to exchange reactive and real power with the system. It does so in response to the systems compensation needs, thereby improving system stability. The STATCOM achieves this by reducing low-range frequency oscillations and maintaining the systems voltage level. The VSC connected to the transformers secondary side exchanges actual and reactive power.

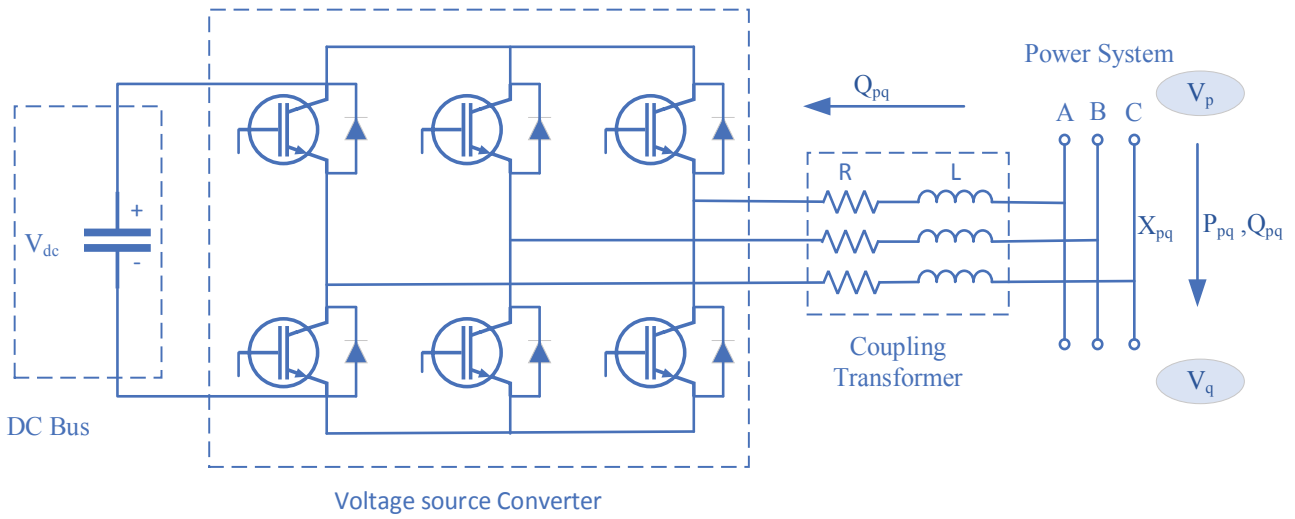


Figure 3. STATCOM with VSC.

The voltage source converter (VSC) comprises a variety of power electronic switching devices, including gate turn-off thyristors (GTOs) and insulated-gate bipolar transistors (IGBTs), which are a type of forced commutated device.

Now,

$$\text{Active Power, } P_{pq} = \frac{V_p V_q}{X_{pq}} \sin \delta \quad (23)$$

$$\text{Reactive Power, } Q_{pq} = \frac{V_p(V_p - V_q \cos \delta)}{X_{pq}} \quad (24)$$

Here,

V_p - terminal voltage of power system

V_q - VSC terminal voltage

X_{pq} - Reactance to be transferred between the sources

δ - Phase angle between V_p and V_q .

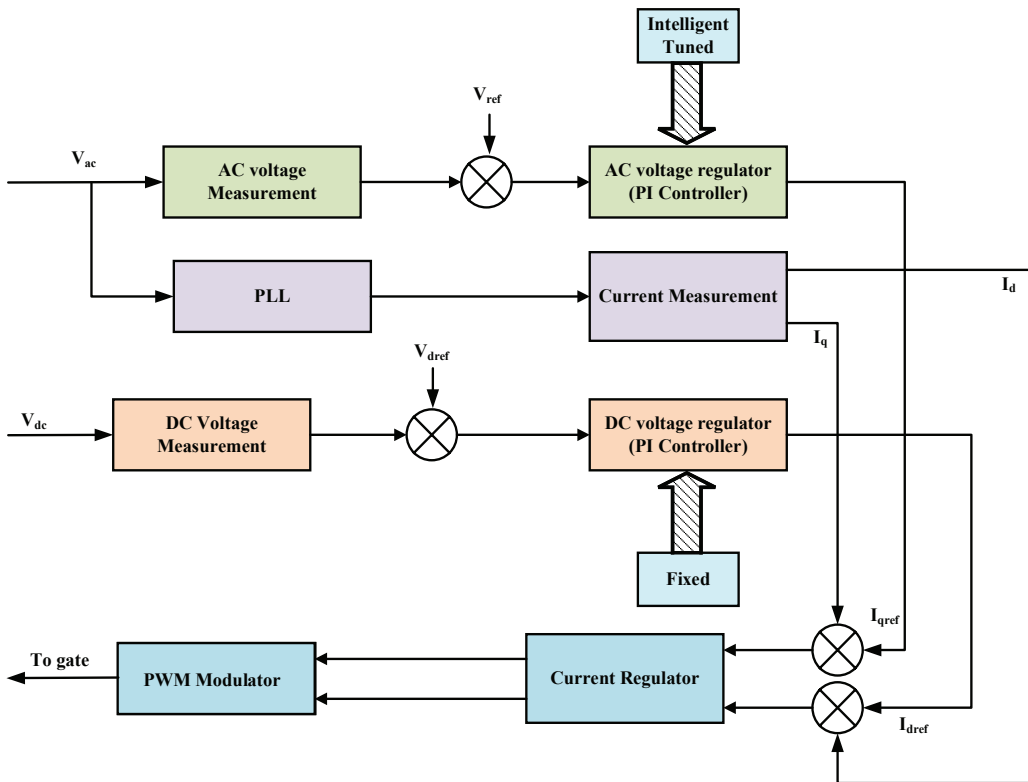


Figure 4. Intelligent-based STATCOM controller.

Under normal circumstances, the voltage V_q generated by the VSC aligns with the system voltage V_p (with a phase angle of $\delta=0$), resulting in the exchange of only lagging VAR (reactive power) and no active power ($P_{pq} = 0$). If the voltage V_p is higher than the voltage V_q , a reactive power flow is initiated from bus of V_p to V_q , as shown in Figure. 3. This occurs when the STATCOM consumes the reactive power, causing it to function as a reactor.

Conversely, when V_p is less than V_q , it indicates that reactive power is transferred from bus of V_q to V_p (STATCOM acts as a capacitor and starts injecting reactive power). The capacitor on the direct current (DC) side of the voltage source converter (VSC) functions as a rigid DC voltage source. Under typical operating conditions, the voltage V_p must lead the voltage that exists V_q to offset losses in the transformer and voltage source converter (VSC) and to maintain a charged capacitor.

The synchronously rotating d-q frame model can be used to describe the STATCOM in the following manner:

$$\frac{di_{sd}}{dt} = \frac{-R_s \omega_0}{X_s} i_{sd} - \omega_0 i_{sq} + \frac{\omega_0}{X_s} (v_{1d} - v_{2d}) \quad (25)$$

$$\frac{di_{sq}}{dt} = \omega_0 i_{sd} - \frac{R_s}{X_s} i_{sq} + \frac{\omega_0}{X_s} (v_{1q} - v_{2q}) \quad (26)$$

$$\frac{dv_{dc}}{dt} = \frac{-P_s}{Cv_{dc}} - \frac{v_{dc}}{R_c C} \quad (27)$$

Here, “ i_{sd} ” and “ i_{sq} ” stand for the STATCOM’s current d-q frame components. the current components of the STATCOM in the d-q frame, ω_0 is the angular velocity, R_s and X_s stand for the coupling transformer’s resistance and leakage reactance, and capacitor shunt’s leakage resistance is denoted as R_c .

The proposed study utilizes Voltage Source Converters (VSC) that consist of Insulated Gate Bipolar Transistor (IGBT)-based Pulse Width Modulation (PWM) inverters. These inverters operate at a chopping frequency in the kilohertz range and employ the PWM approach to generate a sinusoidal waveform using a direct current (DC) voltage source. The filters attached to the VSC’s AC end neutralize voltage harmonics. By adjusting the PWM-modulator’s modulation index, the VSC can extract the voltage V_2 from a constant DC voltage V_{dc} . The gate pulses needed to switch and regulate the IGBTs used in the VSC are provided by the PWM generator. The suggested control technique uses PLL (Phase-locked loop) to output d and q-axis current components I_d and I_q from transmission line AC voltage. Additionally, two PI controllers, one for AC and one for DC, help minimize AC and DC current errors. The reference currents for these controllers are the quadrature axis currents, I_q , and I_d , as well as the direct current. The current regulator is employed to govern the gate signal generated

by the PWM converter by utilizing reference currents I_{dref} and I_{qref} offered by the DC and AC voltage regulators, respectively. The gate signal further synthesizes the voltage V_2 ’s phase and magnitude (V_{2d} , V_{2q}). Soft computing optimization techniques are employed to adjust the gain parameters PI of the AC controllers by the system needs, while the PI value of the DC controllers remains constant. Figure 4. depicts the comprehensive schematic representation of the proposed controller.

PARTICLE SWARM OPTIMIZATION (PSO) ALGORITHM

Particle Swarm Optimization (PSO) involves moving a group of potential solutions, particles, within the search space to locate the most optimal solution. The position of each particle within the solution space indicates a potential solution, and its mobility is impacted by both its own personal best position and the best position discovered by the entire swarm.

The algorithm’s key components involve updating the velocity and position of each particle in each iteration. The particles adapt their locations according to their previous encounters. and the global best solution discovered by any particle in the swarm. The flowchart depicting the PSO algorithm is depicted in Figure 5, while its Parameters are outlined in Table 2. Which are determined through a review of relevant literature [29] and experimentation to

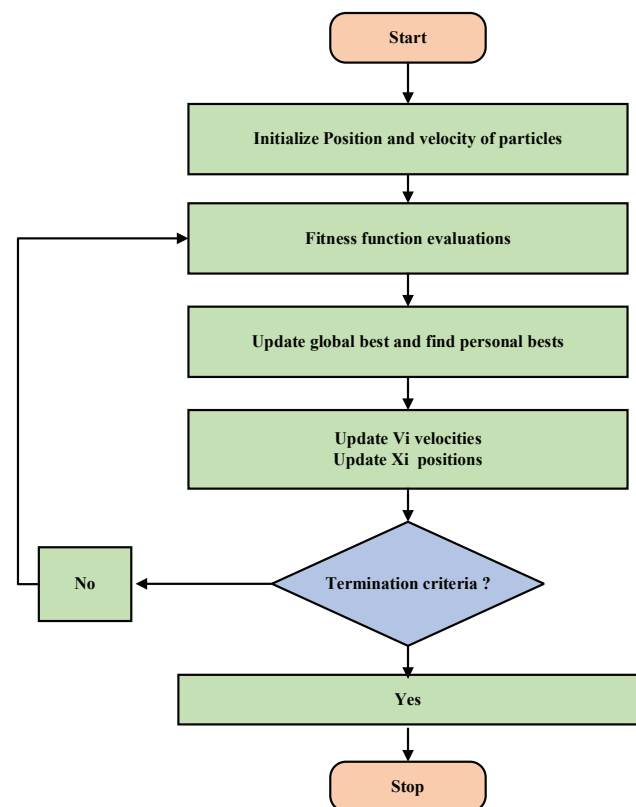


Figure 5. Flowchart of PSO.

Table 2. Parameters of PSO

Parameters	Number of variables	Population size	Generation	Weighing factor	pbest and gbest	Maximum inertia weight	Minimum inertia weight	Cognitive and Social Parameters (c1, c2)
Values	2 (K_p, K_i)	100	10	0.9	2.5	0.9	0.2	2

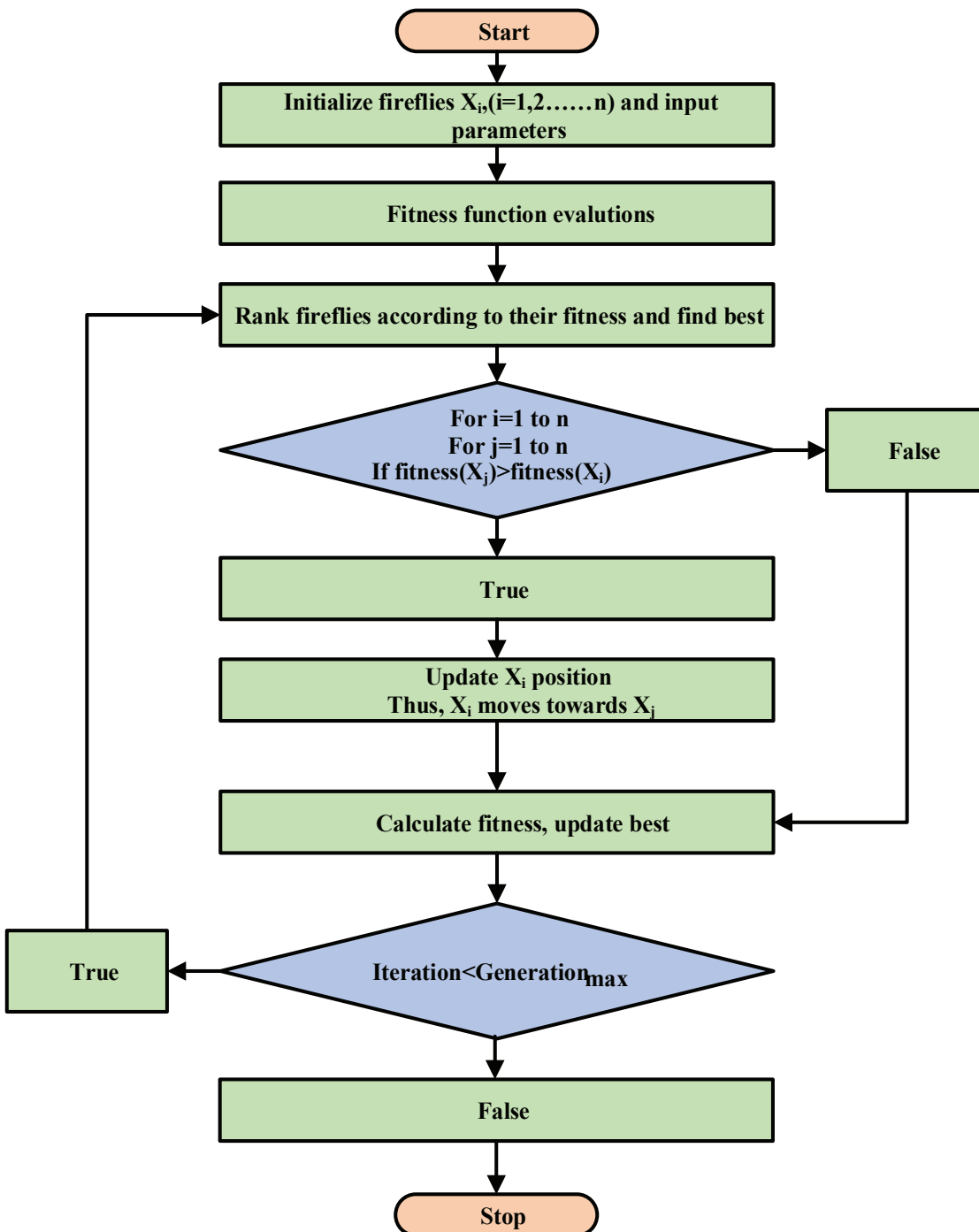


Figure 6. Flowchart of fireflies.

Table 3. Parameters of Firefly

Parameters	No of variables	Number of Fireflies	Light Absorption Coefficient	No of iteration	Alpha (Randomization parameter)	Beta (Initial Attractiveness)	Gamma (Absorption coefficient)
Values	2 (K_p, K_i)	20	1	100	0.4	1	2

ensure optimal performance. This cooperative exploration of the solution space allows PSOs to navigate toward promising regions efficiently.

The simplicity and efficiency of PSO make it well-suited for a broad spectrum of optimization issues. Its intuitive nature and ease of implementation have contributed to its popularity in various fields, including engineering [30,31], finance, and artificial intelligence. Despite its simplicity, PSO has proven to be a powerful tool for finding optimal solutions in complex, multi-dimensional search spaces.

FIREFLIES ALGORITHM

Fireflies, scientifically known as Lampyridae, are nocturnal beetles renowned for their bioluminescent glow. They use this light primarily for communication and mating, with males emitting rhythmic flashes to attract females, each species having its unique pattern. Additionally, the glow serves as a defense mechanism, warning predators of their unpalatability. Beyond their natural behaviors, fireflies inspire scientific and technological advancements.

Overall, fireflies are captivating creatures that contribute to the natural beauty of their habitats and scientific advancements, making them a subject of interest and admiration in biological and technological contexts [30], [31]. The flow chart of FF is depicted in Figure 6, while its parameters are outlined in Table 3 [29].

GREY WOLF OPTIMIZER (GWO)

The Grey Wolf Optimizer (GWO) is an optimization algorithm that draws inspiration from the social structure and hunting behavior of grey wolves in nature. Introduced in 2014 by Mirjalili et al., GWO has gained popularity as a robust optimization algorithm in various fields.

Inspired by the cooperative nature of wolf packs, GWO divides the optimization process into three key phases: encircling, attacking, and updating. In the encircling phase, the positions of alpha (m), beta(n), and delta (o) wolves represent potential solutions. These wolves emulate the leadership hierarchy within a wolf pack. The algorithm then employs equations derived from the hunting behavior of wolves to update the positions of the m , n , and o wolves during the attacking phase[32].

Algorithm Steps:

Step 1: Initialization: Generate a population of grey wolves, each representing a potential solution to the optimization problem. Assign each wolf a position in the search space.

Step 2: Objective Function: Determine the fitness of each wolf by applying the objective function to its position in the search space.

Step 3: Update Alpha, Beta, and Delta Wolves: Identify the alpha, beta, and delta wolves based on their fitness. These wolves represent the best, second-best, and third-best fitness, respectively.

Step 4: Update Positions: Use mathematical transformations to update the positions of the alpha, beta, and delta wolves. Encourage exploration by adjusting the positions based on random values and the difference between wolves.

Step 5: Update Other Wolves: Update the positions of the remaining wolves based on the positions of the alpha, beta, and delta wolves. This step encourages the entire population to converge towards better solutions.

Step 6: Boundary Checking: Ensure that the updated positions of wolves are within the specified search space. If a wolf goes beyond the boundaries, bring it back.

Step 7: Repeat: Reiterate steps 2-6 for a specified quantity of repetitions or until a convergence requirement is achieved.

The algorithm maintains a balance between exploration and exploitation. The alpha, beta, and delta wolves guide the search, exploring new regions, while the rest of the pack follows to exploit promising areas. The mathematical transformations introduce randomness and diversity, preventing premature convergence and encouraging global exploration. The GWO algorithm is versatile and can be applied to various optimization problems by customizing the objective function. The Pseudo code is described in Figure 7.

```

Initialize the grey wolf population  $X_a(a=1,2,3,...n)$ 
Initialize a, A, and C
Calculate the fitness of each search agent
 $X_m$ =the best search agent
 $X_n$ =the second best search agent
 $X_o$ =the third best search agent
While ( $t < \text{Max number of iterations}$ )
  for each search agent
    Update the position of current search agent by equation (40)
  end
  Update a, A, and C
  Calculate the fitness of all search agents
  Update  $X_m$ ,  $X_n$  and  $X_o$ 
   $t=t+1$ 
end while
return  $X_m$ 

```

Figure 7. Pseudo code of GWO algorithm.

Table 4. Parameters of GWO

Parameters	No of variables	No of iteration	Number of search Agents	Position vector	Control Vector (a)
Values	2 (Kp, Ki)	100	20	Rand	Lies between 2 and 0

Mathematical Model

An outline of the Grey Wolf Optimizer (GWO) algorithm follows the presentation of the mathematical models for tracking, surrounding, attacking, and social hierarchy in this section.

$$\vec{D}_n = |\vec{C}_b \cdot \vec{X}_n - \vec{X}| \quad (35)$$

$$\vec{D}_o = |\vec{C}_c \cdot \vec{X}_o - \vec{X}| \quad (36)$$

Social Hierarchy

In the mathematical model of the social structure of wolves in the GWO, the strongest and most resilient solution is represented as alpha (m). Conversely, the solutions ranked second and third are denoted as beta (n) and delta (o) correspondingly. Other candidate solutions are denoted as omega (x). The optimization process is guided by m, n, and o, with the remaining wolves following their lead.

$$X_a = \vec{X}_m - \vec{A}_a \cdot (\vec{D}_m) \quad (37)$$

$$\vec{X}_b = \vec{X}_n - \vec{A}_b \cdot (\vec{D}_n) \quad (38)$$

$$\vec{X}_c = \vec{X}_o - \vec{A}_c \cdot (\vec{D}_o) \quad (39)$$

Encircling Prey

Grey wolves exhibit encircling behavior during hunting. The mathematical representation of this behavior is described by the following equations:

$$\vec{D} = |\vec{C} \cdot \vec{X}_o(k) - \vec{X}(k)| \quad (30)$$

$$\vec{X}(k+1) = \vec{X}_o(k) - \vec{A} \cdot \vec{D} \quad (31)$$

In this context, the variable k represents the current iteration, whereas \vec{A} and \vec{C} are coefficient vectors. \vec{X}_o refers to the position vectors of the prey, while \vec{X} represents the position vector of a grey wolf. The vectors \vec{A} and \vec{C} are calculated using specific formulas involving random vectors.

$$\vec{A} = 2\vec{a} \cdot \vec{r}_1 - \vec{a} \quad (32)$$

$$\vec{C} = 2 \cdot \vec{r}_2 \quad (33)$$

Hunting

Grey wolves, guided by alpha, exhibit hunting behavior. To simulate this behavior mathematically, the positions of the m (alpha), n (beta), and o (delta) wolves are considered more informed about the potential prey location. The positions of other wolves, including the omegas, are then updated based on these informed positions:

$$\vec{D}_m = |\vec{C}_a \cdot \vec{X}_m - \vec{X}| \quad (34)$$

This approach ensures that the search agents, except for the top three, update their positions according to the more knowledgeable alpha, beta, and delta wolves. These mathematical formulations and algorithms capture the essence of the GWO, where social hierarchy, encircling prey, and hunting behaviors are translated into mathematical models for optimization purposes.

The proposed study includes a flow chart of the Grey Wolf Optimizer (GWO), which is depicted in Figure 8. and its parameters are described in Table 4. The AC PI controllers' gain parameters are modified by applying soft computing optimization approaches to diminish deviations in rotor dynamics, specifically generator speed deviation, LP turbine speed deviation, HP turbine speed deviation, torque deviation in LP-HP turbine, and torque deviation in the generator. The performance indices, i.e., ITAE criteria is considered for the above optimization technique used:

$$ITAE = \int_0^t (|\Delta\omega_{GEN}| + |\Delta\omega_{LPT}| + |\Delta\omega_{HPT}| + |\Delta\tau_{GEN}| + |\Delta\tau_{LPT-HPT}|) dt \quad (41)$$

To get the best values for the AC PI controllers' gain settings, we first use the hit-trial method to initialize them. Depending on the precise location (Particles, Fireflies, wolf), the PI controllers' gain values are determined in optimization. The area is dependent on the chosen technique. When you update that position, the AC PI controllers' corresponding gain values are updated, but the DC PI controllers' gain values remain unchanged.

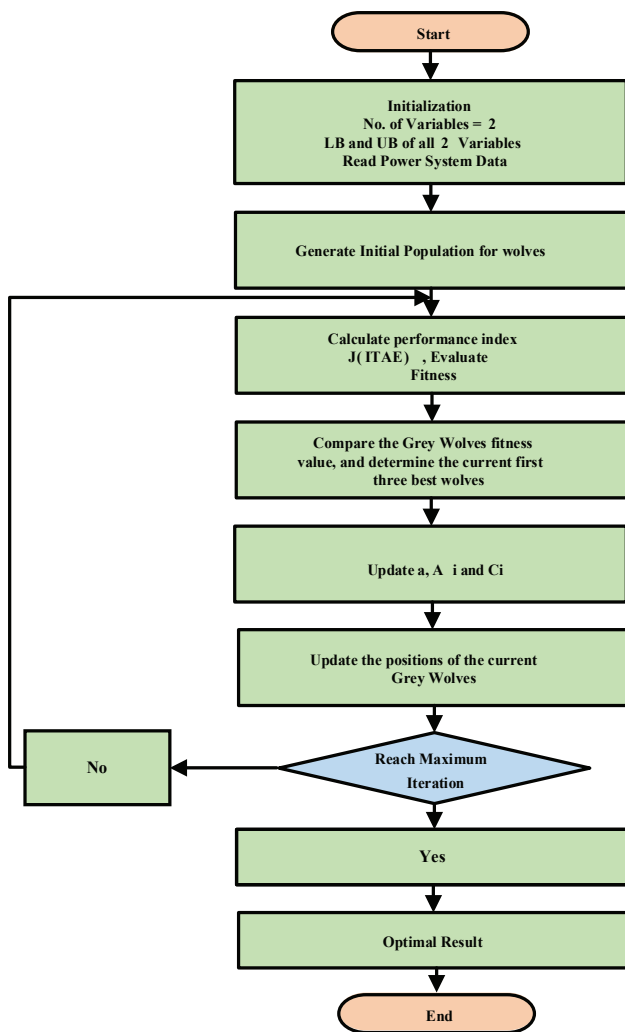


Figure 8. Flowchart of GWO in the proposed study.

RESULTS AND DISCUSSION

In this study, the VSC-based STATCOM is employed to mitigate sub-synchronous oscillations within the IEEE SBM test system. These oscillations pose a significant risk of system disturbances, particularly if they lead to cascading line outages due to oscillatory swings among interconnected components. Utilizing MATLAB software, we simulate the test system to analyze rotor dynamics, focusing on deviations in generator speed, LP and HP turbine speeds, as well as torque fluctuations in the generator and LP-HP turbine. The results obtained from analyzing the rotor dynamics of all the machines under different test scenarios, such as without STATCOM, with STATCOM, and with the proposed intelligently tuned STATCOM controller, clearly demonstrate the effectiveness of the optimization-based control scheme in alleviating sub-synchronous oscillations in the power system when integrated with the STATCOM.

A MATLAB GUI (guided user interface) has been created to enhance the visualization of simulation

outcomes and key system parameters. This encompasses specific information like as the generators MVA (Mega Volt Ampere) and kV (kilo Volt) rating, timing of faults, reference voltage, and the introduction of disturbances, particularly system damping. If the system's natural dampings are not taken into account, the GUI will receive a zero input. This means that if the natural dampings are zero, the input will be one when the natural damping is considered.

Case A: System Results with Zero Damping

The test system comprises an alternator with a rating of 600 MVA and 22 kV. The system experiences a 3-phase LLL-G fault, with natural damping zero. The rotor dynamics, i.e., fluctuations in generator LP Turbine, HP turbine, is shown in the Figure 9, 10, and 11, respectively, while the amplification of torque in LP-HP turbine and generator is in the Figure 12 and 13.

The system under investigation's characteristics is assessed for a duration of 5 seconds based on its transient response. In Table 5, outlining settling times (in seconds) for quantities without natural damping, a comparative analysis of PSO, FF, and GWO controllers against the reference STATCOM is presented. For Generator Speed deviation, all three controllers exhibit improvements over STATCOM (3.9942 seconds), with PSO-STATCOM, FF-STATCOM, and GWO-STATCOM achieving reductions of approximately 17.3%, 17.0%, and 17.7%, respectively. Similarly, for LP Turbine Speed deviation, the controllers showcase notable percentage reductions compared to STATCOM alone (3.8901 seconds), with PSO-STATCOM, FF-STATCOM, and GWO-STATCOM achieving decreases of approximately 13.7%, 13.6%, and 13.4%, respectively. Analyzing HP Turbine Speed deviation, all controllers outperform STATCOM (3.9731 seconds) with percentage reductions of approximately 17.7%, 25.0%, and 18.1% for PSO-STATCOM, FF-STATCOM, and GWO-STATCOM, respectively. Examining Torque deviation in LP-HP Turbine, all three controllers significantly reduce settling times compared to STATCOM (4.1092 seconds) with improvements of approximately 32.1%, 32.0%, and 32.9% for PSO-STATCOM, FF-STATCOM, and GWO-STATCOM, respectively. For Torque deviation in the Generator, the controllers demonstrate substantial percentage improvements over STATCOM alone (4.1087 seconds), with reductions of approximately 32.0%, 32.8%, and 33.8% for PSO-STATCOM, FF-STATCOM, and GWO-STATCOM, respectively.

In summary, PSO, FF, and GWO controllers consistently outperform STATCOM across various quantities, showcasing their effectiveness in reducing settling times and enhancing system dynamics. GWO-STATCOM generally exhibits slightly superior performance regarding percentage reduction in settling time.

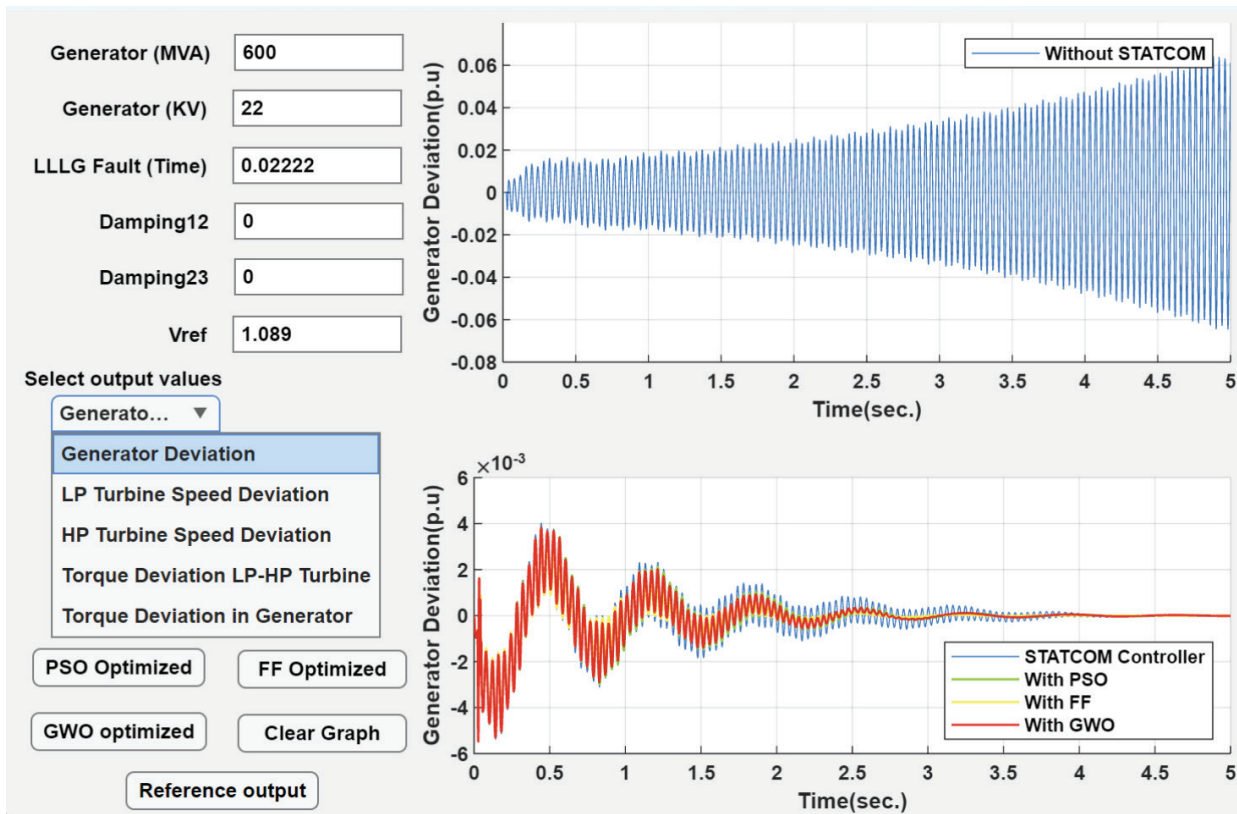


Figure 9. Fluctuation in the generator of case A.

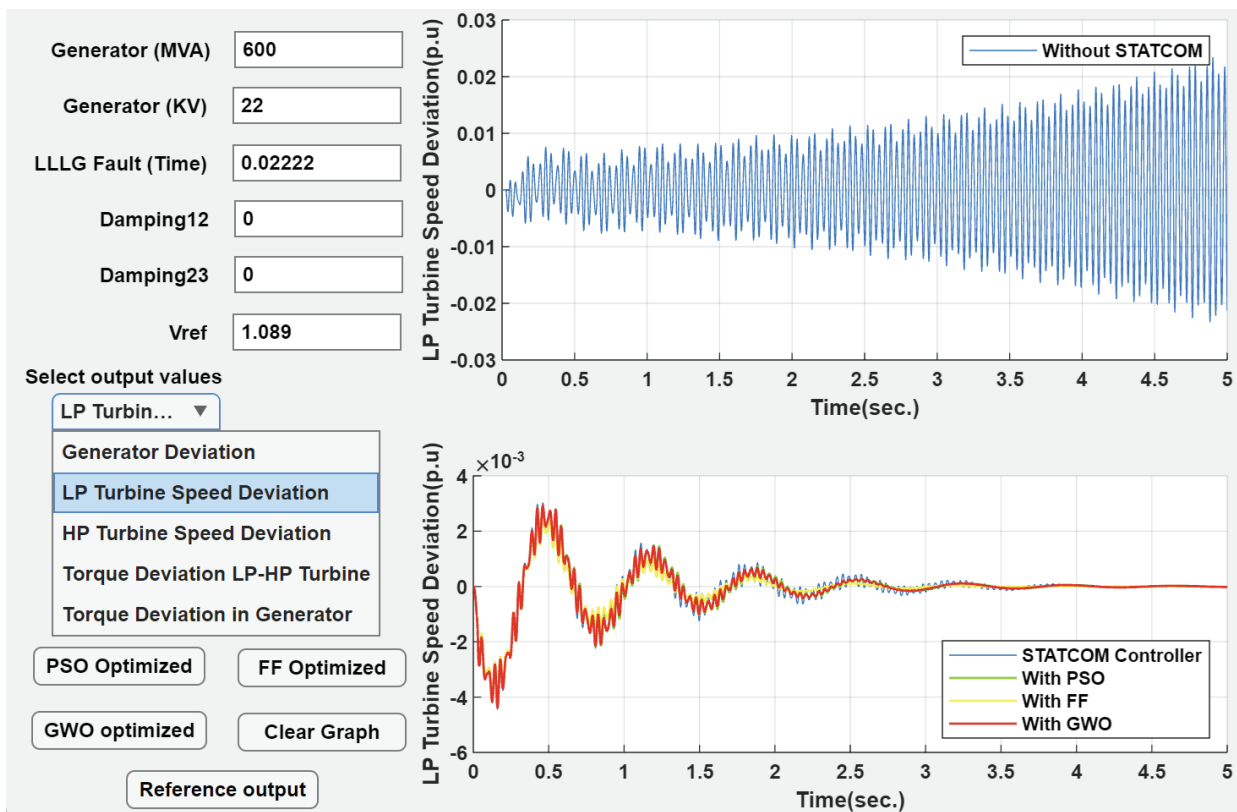


Figure 10. Fluctuation in LP Turbine of case A.

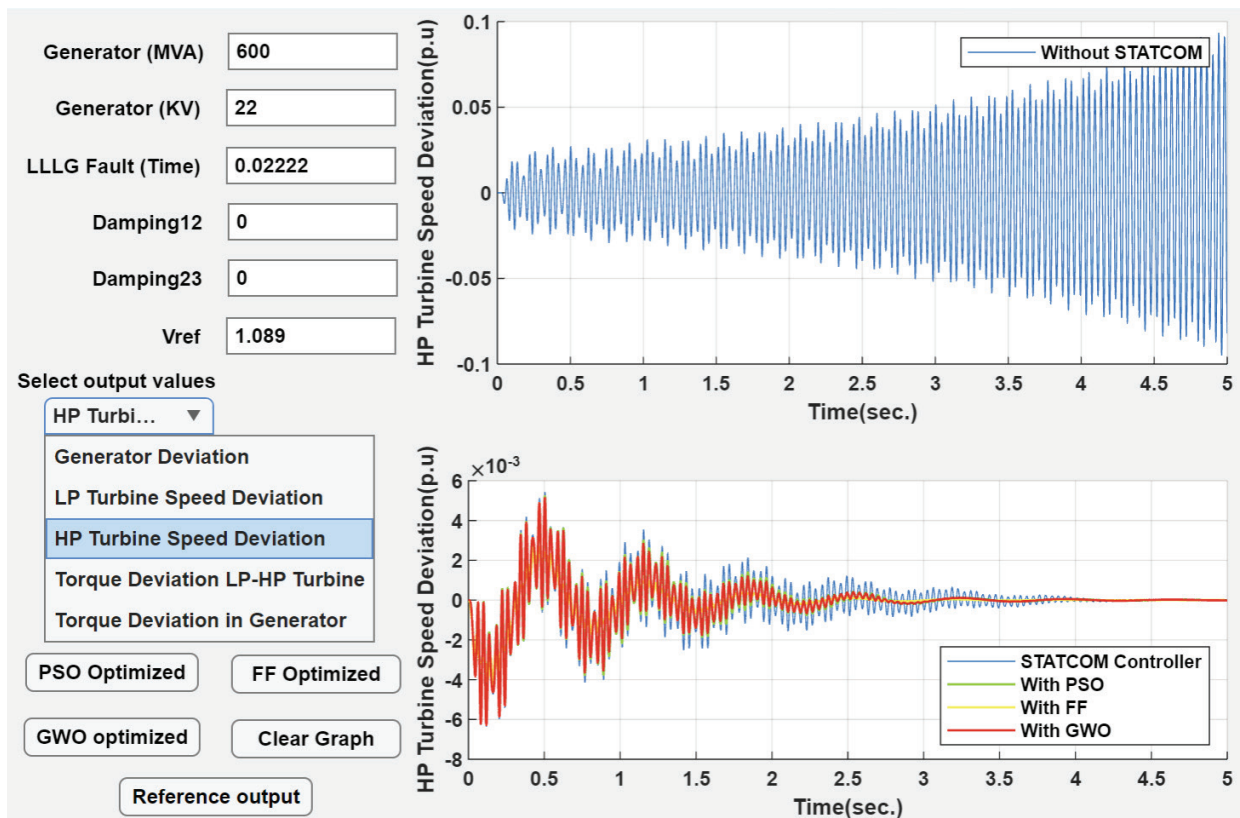


Figure 11. Fluctuation in HP Turbine of case A.

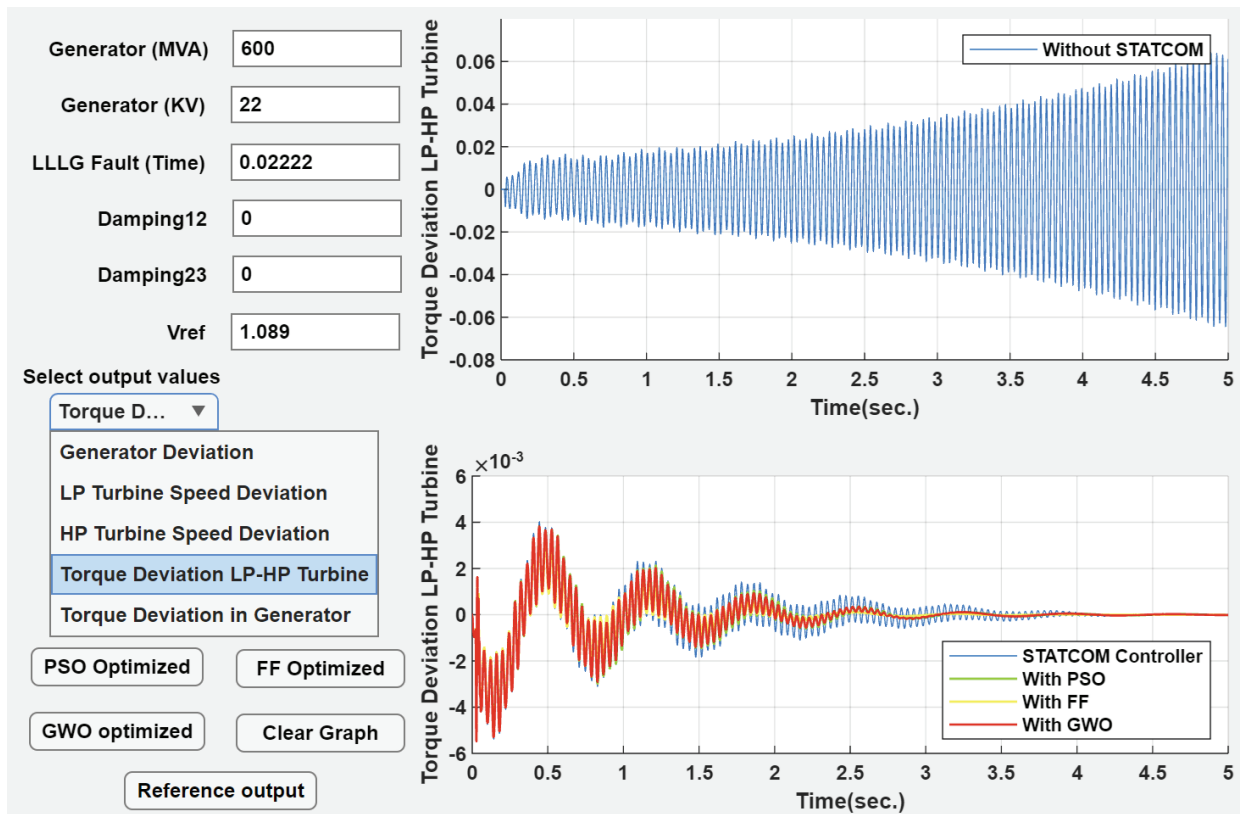


Figure 12. Amplification of Torque in LP-HP Turbine of Case A.

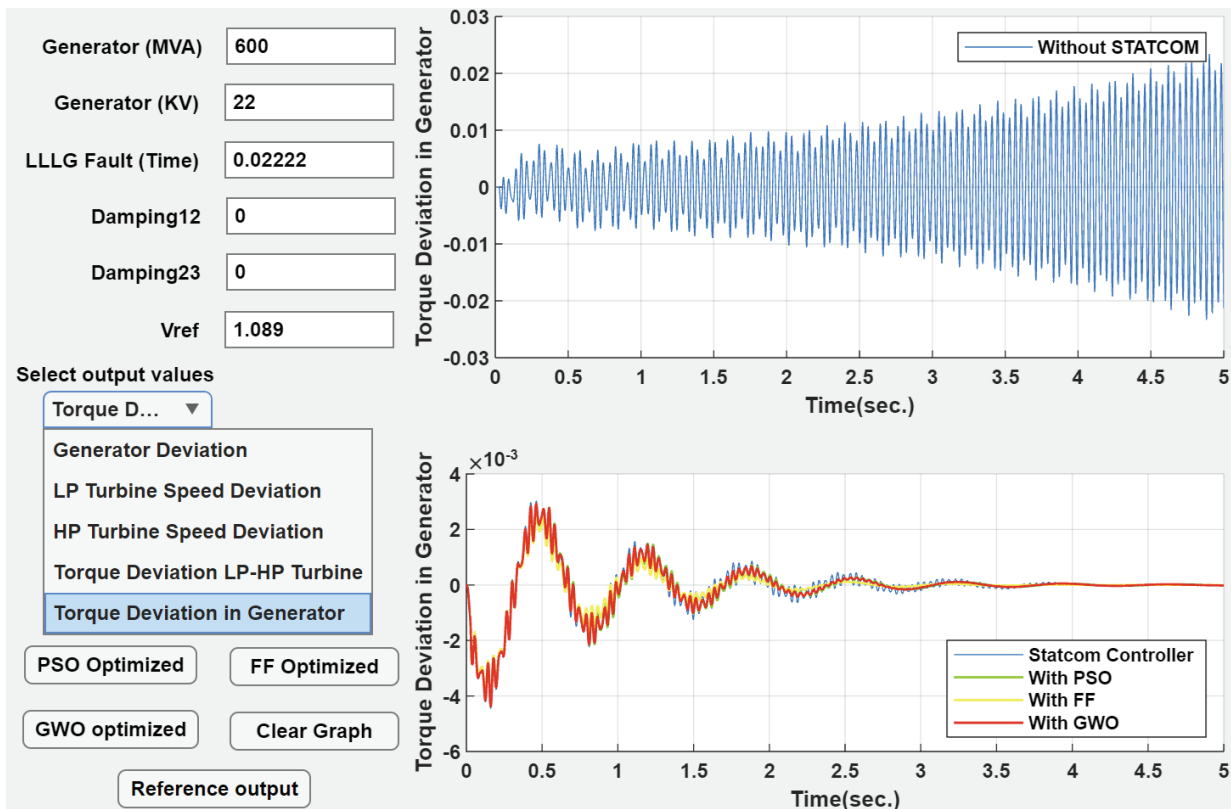


Figure 13. Amplification of Torque in Generator of Case A.

Table 5. Time domain specifications (Settling time in sec.) of the Quantities without natural damping

Quantity	Without STATCOM	With STATCOM	With PSO-STATCOM controller	With FF-STATCOM controller	With GWO-STATCOM controller
Generator Speed deviation	Unspecified	3.9942	3.3017	3.3149	3.2928
LP Turbine speed deviation	Unspecified	3.8901	3.3549	3.3571	3.3390
HP Turbine speed deviation	Unspecified	3.9731	3.2701	2.9852	3.2504
Torque deviation in LP-HP Turbine	Unspecified	4.1092	2.7971	2.7941	2.7575
Torque deviation in generator	Unspecified	4.1087	2.7960	2.7572	2.7183

Case B: System Results with Natural Damping

The system's response is illustrated after applying a three-phase LLL-G fault, taking into account inherent damping effects. Figures 14, 15, and 16 illustrate the fluctuations observed in the generator, LP turbine, and HP turbine, respectively. Additionally, Figures 17 and 18 demonstrate the amplification of torque in the LP-HP turbine and generator, respectively.

In Table 6, presenting settling times (in seconds) for quantities with natural damping, we compare the performance of PSO, FF, and GWO controllers against the baseline STATCOM. For the Generator Speed deviation, all three controllers show significant improvements compared to STATCOM alone (3.1855 seconds). PSO-STATCOM

achieves a reduction of approximately 19.3%, FF-STATCOM demonstrates a decrease of about 20.0%, and GWO-STATCOM provides a notable improvement of around 20.0%. Similarly, the controllers exhibit commendable reductions for LP Turbine Speed deviation compared to the baseline (2.9350 seconds with STATCOM). PSO-STATCOM, FF-STATCOM, and GWO-STATCOM achieved percentage improvements of approximately 11.3%, 11.5%, and 12.1%, respectively. For HP Turbine Speed deviation, all controllers outperform STATCOM alone (3.2061 seconds), with PSO-STATCOM, FF-STATCOM, and GWO-STATCOM showing percentage reductions of approximately 20.4%, 21.4%, and 21.6%, respectively. Analysing Torque deviation in LP-HP Turbine, all three controllers significantly

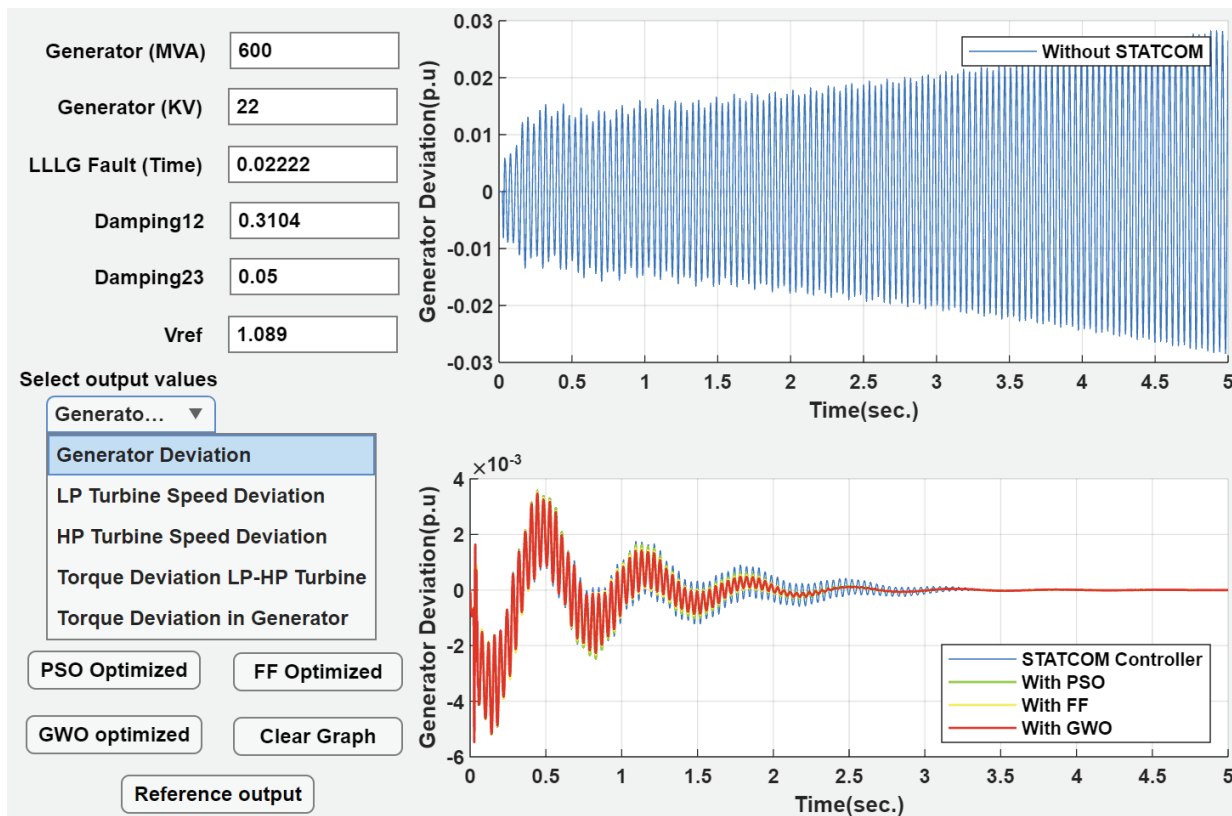


Figure 14. Fluctuation in the generator of case B.

Table 6. Time domain specifications (Settling time in sec.) of the Quantities with natural damping (D12=0.3104, D23=0.05)

Quantity	Without STATCOM [23]	With STATCOM [33]	With PSO-STATCOM controller	With FF-STATCOM controller	With GWO-STATCOM controller
Generator Speed deviation	Unspecified	3.1855	2.5790	2.5491	2.5488
LP Turbine speed deviation	Unspecified	2.9350	2.6018	2.5902	2.5828
HP Turbine speed deviation	Unspecified	3.2061	2.5572	2.5237	2.5231
Torque deviation in LP-HP Turbine	Unspecified	3.2377	2.3724	2.3363	2.3352
Torque deviation in generator	Unspecified	3.2801	2.3721	2.3349	2.3339

improve settling times compared to STATCOM (3.2377 seconds). PSO-STATCOM, FF-STATCOM, and GWO-STATCOM demonstrate percentage reductions of approximately 26.7%, 27.0%, and 27.3%, respectively. Finally, for Torque deviation in the Generator, the controllers exhibit notable reductions compared to STATCOM alone (3.2801 seconds). PSO-STATCOM, FF-STATCOM, and GWO-STATCOM achieved percentage improvements of approximately 27.7%, 27.8%, and 27.9%, respectively.

In summary, PSO, FF, and GWO controllers consistently outperform STATCOM across various quantities, showcasing their effectiveness in reducing settling times and enhancing system dynamics. GWO-STATCOM generally

exhibits slightly superior performance regarding percentage reduction in settling time.

Table 7 presents a comparative analysis of STATCOM performance and is refined through various tuning methodologies – PSO, FF, and GWO while excluding natural damping effects. The Integral of Time Absolute Error (ITAE) improvement is assessed in percentage terms concerning the original STATCOM parameters ($K_p = 5$, $K_i = 1000$). PSO tuning resulted in a 30.5% enhancement, adjusting K_p to 9.2516 and K_i to -1244.8446. The FF-tuned configuration exhibited a 32.0% improvement, with K_p and K_i values adjusted to 12.2376 and 2.3144, respectively. GWO tuning yielded a 33.5% enhancement, setting K_p and K_i to 7.3691 and -1932.6593. These results highlight

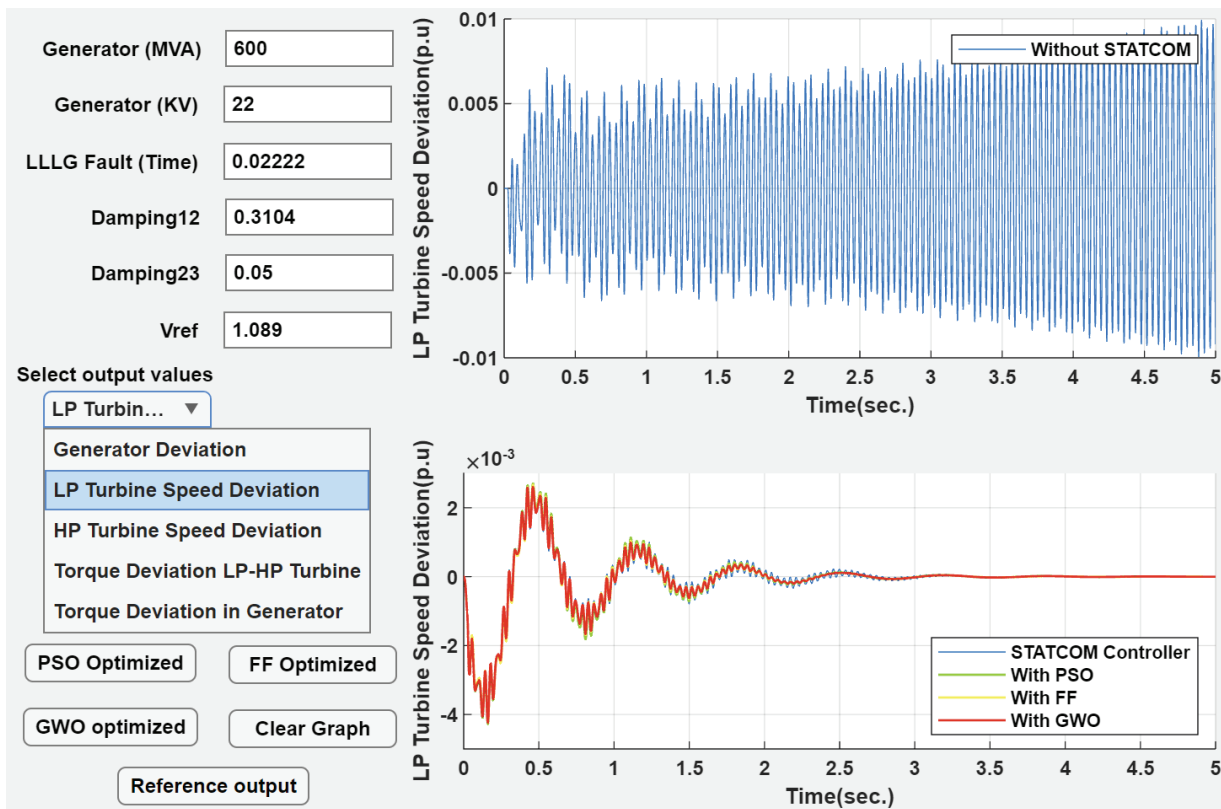


Figure 15. Fluctuation in LP Turbine of case B.

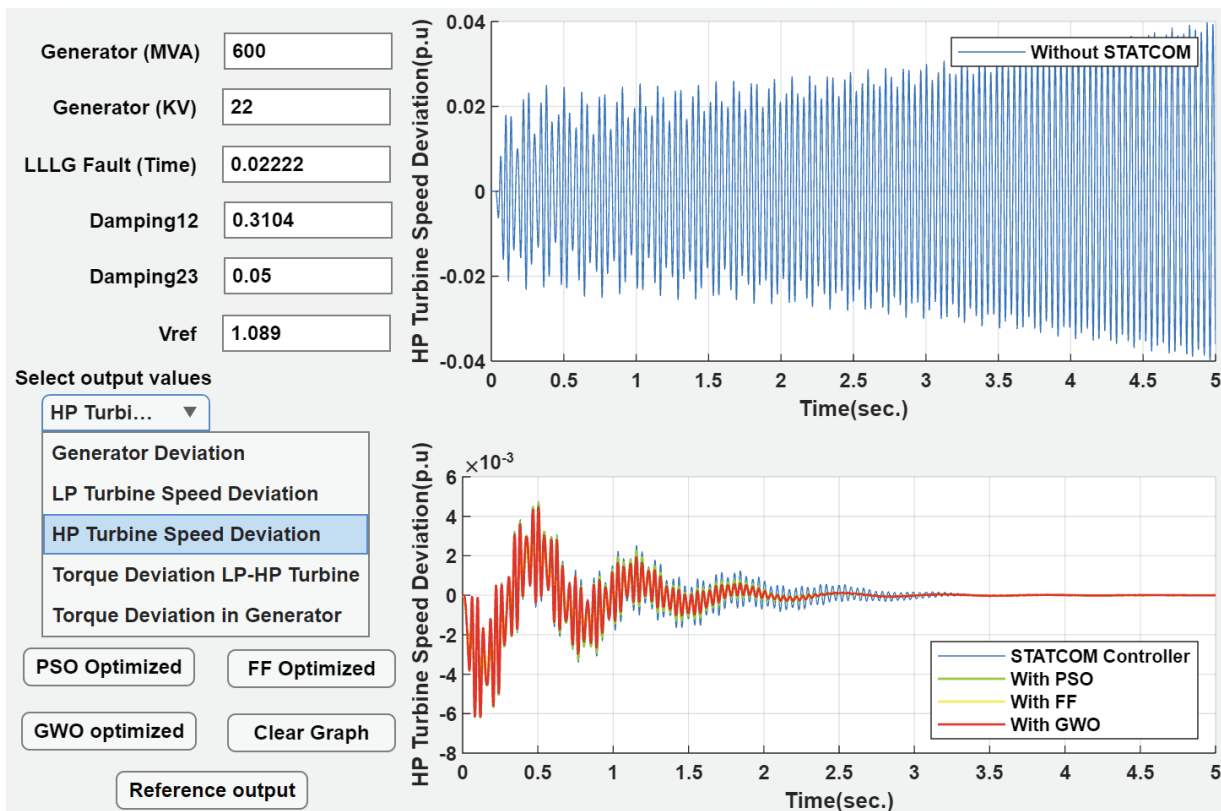


Figure 16. Fluctuation in HP Turbine of case B.

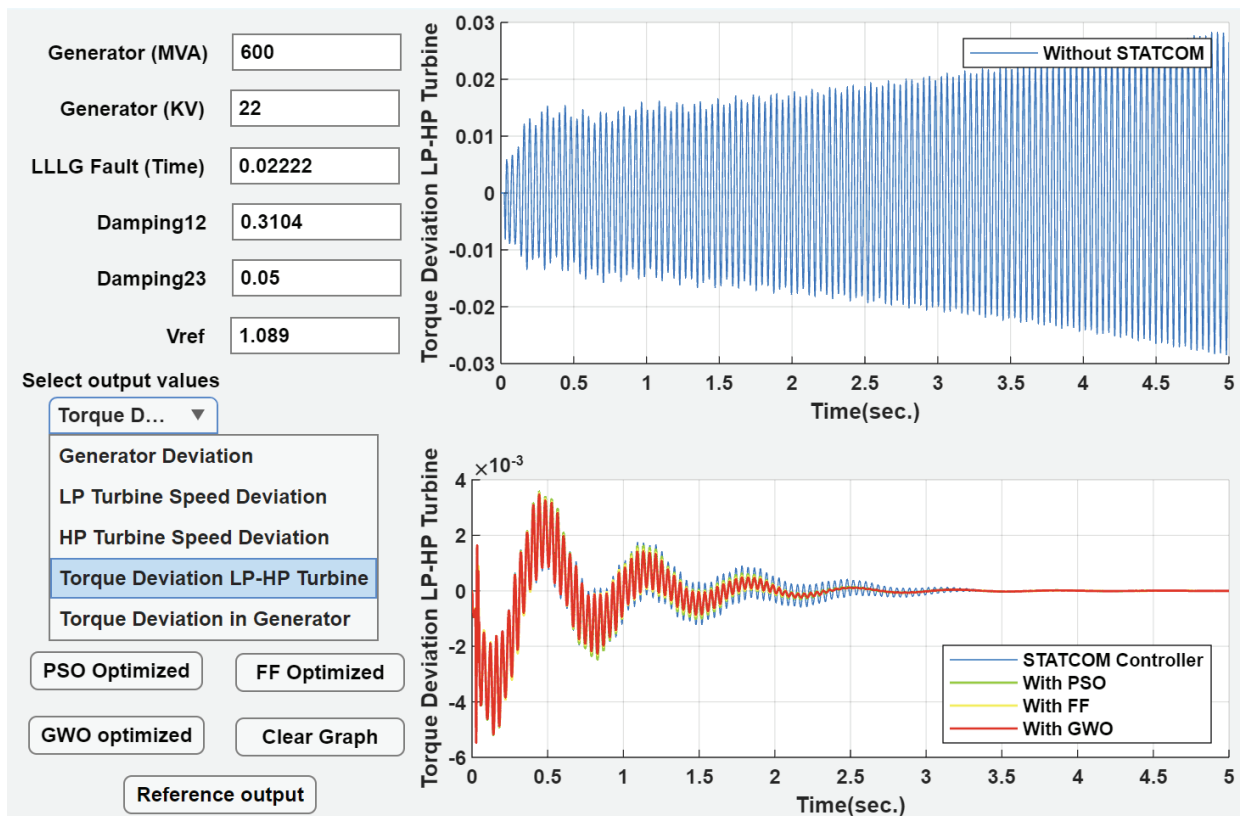


Figure 17. Amplification of Torque in LP-HP Turbine of Case B.

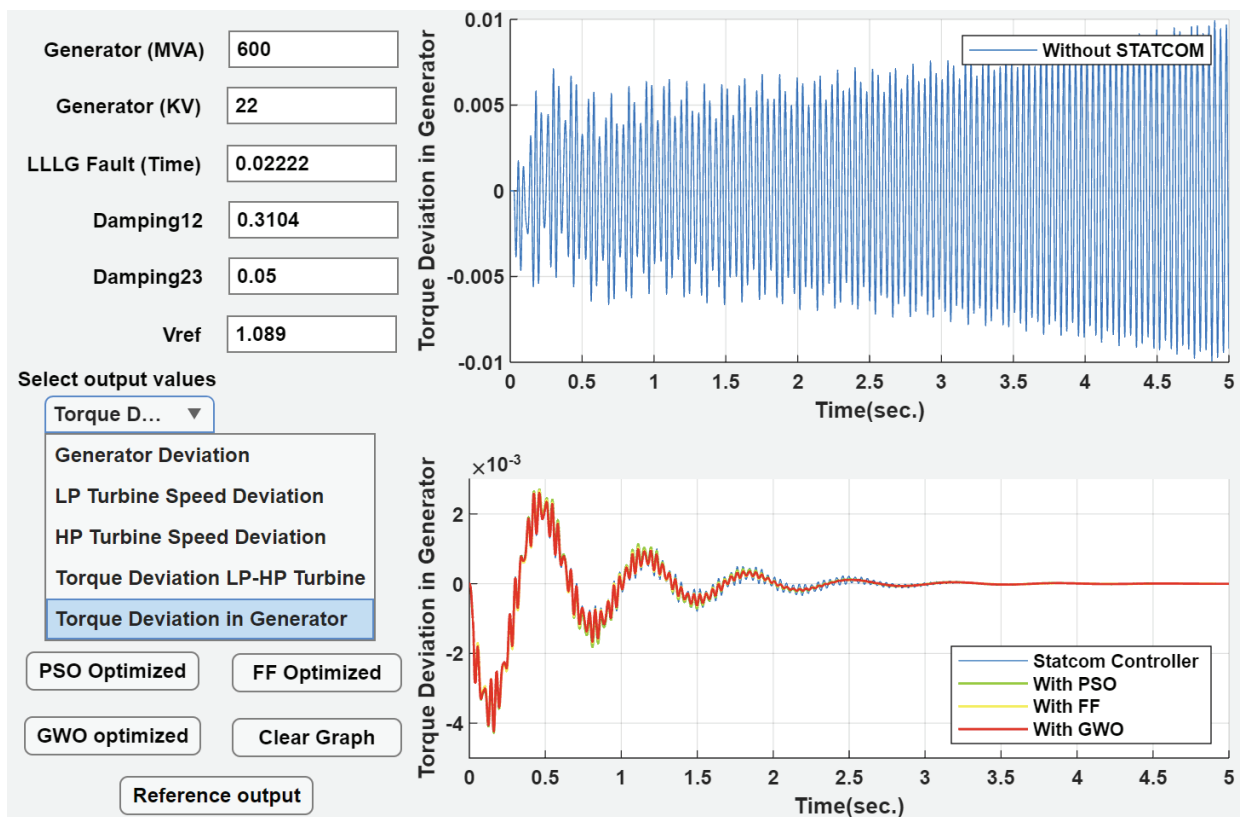


Figure 18 Amplification of Torque in Generator of Case B.

Table 7. Comparative Parameters assessment of STATCOM refined through FF, GWO, and PSO tuning methodologies without natural damping

Quantity	K_p	K_i	ITAE
ONLY STATCOM	5	1000	0.4542
PSO tuned STATCOM	9.2516	-1244.8446	0.3153
FF tuned STATCOM	12.2376014396766	2.31441600588101	0.3087
GWO tuned STATCOM	7.3691	-1932.6593	0.3023

Table 8. Comparative Parameters assessment of STATCOM, refined through FF, GWO, and PSO tuning methodologies with natural damping

Quantity	K_p	K_i	ITAE
ONLY STATCOM	5	1000	0.3070
PSO tuned STATCOM	2.2865	147.6050	0.2118
FF tuned STATCOM	20	1201.53262819189	0.2205
GWO tuned STATCOM	-11.9964	299.9140	0.2101

the efficacy of the tuning methodologies in optimizing the STATCOM parameters, showcasing substantial percentage improvements in ITAE, a key indicator of control system performance. These findings underscore the significance of advanced optimization techniques in enhancing the dynamic response of STATCOM systems without natural damping.

Table 8 presents a comparative evaluation of STATCOM performance, considering natural damping effects and refining parameters through FF, GWO, and PSO tuning methodologies. The initial STATCOM configuration with K_p at 5 and K_i at 1000 yielded an ITAE of 0.3070. Following PSO tuning, the system demonstrated a significant 31.0% improvement, with K_p and K_i adjusted to 2.2865 and 147.6050, respectively, resulting in an ITAE of 0.2118. Conversely, the FF-tuned STATCOM exhibited a 28.2% improvement, with K_p set to 20 and K_i to 1201.5326, yielding an ITAE of 0.2205. GWO tuning led to a notable 31.6% enhancement, adjusting K_p to -11.9964 and K_i to 299.9140, resulting in an ITAE of 0.2101. These findings underscore the efficacy of the tuning methodologies in achieving substantial percentage improvements in ITAE, emphasizing their relevance in optimizing the dynamic response of STATCOM systems in the presence of natural damping.

CONCLUSION

In this paper, an investigation is conducted to examine the optimization tuned control system for mitigating sub-synchronous resonance and low-frequency oscillation in a series compensated transmission line completely. The investigation focuses on implementing this control scheme with the VSC-based Static Synchronous Compensator, utilizes the IEEE's second benchmark model, incorporating

a STATCOM at the central bus as the test platform. Intelligent control strategies applied to STATCOM have proven crucial in enhancing power system stability within torsional oscillation environments. By employing Particle Swarm Optimization (PSO), Firefly Algorithm (FF), and Grey Wolf Optimization (GWO) to search for optimal controller parameters, significant advancements are achieved. Particularly, the proposed STATCOM, formulated as an optimization problem and tuned with GWO, exhibits notable advantages over FF, PSO, and standard STATCOM in various rotor dynamics scenarios, including deviations in generator speed low-pressure (LP) and high-pressure (HP) turbine speeds, as well as torque amplification of the generator and LP-HP turbine. The systematic optimization of STATCOM parameters effectively mitigates oscillations, demonstrating its potential to enhance grid resilience. Even under challenging conditions such as zero natural damping and additional perturbations like three-phase LLL-G fault, the proposed GWO Optimization-based STATCOM proves its efficacy through meticulous analysis. This underscores the crucial role of STATCOM control strategies in addressing torsional oscillations, thereby contributing significantly to the dynamic stability of the power system. As the energy landscape continues to evolve, embracing such intelligent technologies becomes imperative for ensuring sustainable and stable power systems.

FUTURE SCOPE

1. Real-Time Implementation: Investigate the feasibility of implementing the proposed controller in real-time power systems, considering practical constraints and ensuring seamless integration with existing infrastructure.

2. Adaptive Control Strategies: Investigate adaptive control systems that can dynamically modify the controller parameters in response to varying system dynamics, providing versatility and adaptability in practical scenarios.
3. Hybrid Approaches: Explore the possibility of merging the capabilities of various optimization techniques or control systems to develop a hybrid solution that utilizes their complementary benefits to enhance performance.
4. Cybersecurity Considerations: Address cybersecurity aspects associated with implementing intelligent control strategies, ensuring the system's resilience against potential cyber threats and attacks.
5. Integration with Renewable Resources: Explore the adaptability of the proposed controller in power systems with a higher penetration of renewable energy sources, considering the unique challenges posed by variable and intermittent generation.
6. Multi-Area Power Systems: Extend the investigation to multi-area power systems to assess the scalability and performance of the proposed controller in more complex grid configurations.
7. Economic Analysis: Perform an economic analysis to examine the cost-effectiveness of implementing the suggested controller in comparison to other options, taking into account the costs associated with installation, maintenance, and operation.

NOMENCLATURE

"H	constant of inertia in MW.s/MVA
K	stiffness in pu torque/electrical rad
D	coefficient of damping in pu torque/pu speed deviation
ω_0	rated speed in electrical rad/s
$\Delta\omega$	speed deviation of mass in pu
ω	speed of a mass in pu
τ	mechanical torques developed by the turbine sections
Δ	small variation from the initial point if prefixed
δ	load angle in rad/s
$\Delta\delta$	twist angle of mass
T_{RP}	speed relay position time constant in the governor
T_{GVR}	governor opening time constant
T_{CHBR}	chamber time constant in front of HP turbine
T_{HL}	HP and LP turbine connection time constant
k_{GVR}	governor system gain constant
F_T	torques in fractions
O_{GVR}	opening of the governor
ORP	speed relay position
X	excitation if subscripted
G	generator, if subscripted
GX	excitation and generator, if subscripted
LPT	low-pressure turbine, if subscripted
LG	low-pressure turbine and generator, if subscripted
HPT	high-pressure turbine, if subscripted

LH	high pressure and low pressure if subscripted
qx	q-axis if subscripted
dx	d-axis if subscripted
aw	armature winding if subscripted
mdx	mutual and d-axis if subscripted
mqx	mutual and q-axis if subscripted
Fd	field winding, if subscripted
DW	damper winding on the d-axis if subscripted
sw	damper winding on the q-axis if subscripted
QW	damper winding on the q-axis if subscripted
dter	terminal and d-axis if subscripted
qter	terminal and q-axis if subscripted
dinf	infinite bus and d-axis if subscripted
qif	infinite bus and q-axis if subscripted
dcp	capacitive and d-axis if subscripted
qcp	capacitive and q-axis if subscripted
i	current in pu
X	reactance in pu
V	voltage in pu
R,r	resistance in pu
Ψ	flux linkage in pu"

AUTHORSHIP CONTRIBUTIONS

Authors equally contributed to this work.

DATA AVAILABILITY STATEMENT

The authors confirm that the data that supports the findings of this study are available within the article. Raw data that support the finding of this study are available from the corresponding author, upon reasonable request.

CONFLICT OF INTEREST

The author declared no potential conflicts of interest with respect to the research, authorship, and/or publication of this article.

ETHICS

There are no ethical issues with the publication of this manuscript.

REFERENCES

- [1] Basler MJ, Basler RC. Understanding power system stability. IEEE Trans Ind Appl 2008;44:463–474. [\[CrossRef\]](#)
- [2] Kundur P. Power System Stability and Control. New York, USA: McGraw Hill;1994.
- [3] Law KT, Godfrey NR. Robust co-ordinated AVR-PSS design. IEEE Trans Power Syst 1994;9:1218–1225. [\[CrossRef\]](#)
- [4] Bourl^os HC, Houry MP. Robust continuous speed governor control for small-signal and transient stability. IEEE Trans Power Syst 1997;12:129–135. [\[CrossRef\]](#)

- [5] Dudgeon GJW, Dysko A, O'Reilly J, McDonald JR. The effective role of AVR and PSS in power systems: Frequency response analysis. *IEEE Trans Power Syst* 2007;22:1986–1994. [\[CrossRef\]](#)
- [6] Wei SZ, Huang Y. Synchronous motor-generator pair to enhance small signal and transient stability of power system with high penetration of renewable energy. *IEEE Access* 2017;5:11505–11512. [\[CrossRef\]](#)
- [7] Xiang JH, Ma J. Distributed power control for transient stability of multimachine power systems. *IEEE J Emerg Sel Top Circuits Syst* 2017;7:383–392. [\[CrossRef\]](#)
- [8] Khayyat-zadeh M, Khayyat-zadeh R. Sub-synchronous resonance damping using high penetration PV plant. *Mech Syst Signal Process* 2017;84:431–444. [\[CrossRef\]](#)
- [9] Varma RK, Varma S. SSR mitigation with a new control of PV solar farm as STATCOM (PV-STATCOM). *IEEE Trans Sustain Energy* 2017;8:1473–1483. [\[CrossRef\]](#)
- [10] Varma RK, Varma H. PV solar system control as STATCOM (PV-STATCOM) for power oscillation damping. *IEEE Trans Sustain Energy* 2019;10:1793–1803. [\[CrossRef\]](#)
- [11] Wang LL, Prokhorov AV, Mokhlis H, Huat CK. Modal control design of damping controllers for thyristor-controlled series capacitor to stabilize common-mode torsional oscillations of a series-capacitor compensated power system. *IEEE Trans Ind Appl* 2019;55:2327–2336. [\[CrossRef\]](#)
- [12] Gupta SK, Gupta AK, Kumar N. Damping subsynchronous resonance in power systems. *IEE Proc Gener Transm Distrib* 2002;149:679–688. [\[CrossRef\]](#)
- [13] Gupta SK, Kumar N, Gupta AK. Controlled series compensation in coordination with double order SVS auxiliary controller and induction M/C for repressing the torsional oscillations in power systems. Available at: www.elsevier.com/locate/epsr Last Accessed Date: 22.11.2024.
- [14] Hingorani NG, Gyugyi L, El-Hawary ME. *Understanding FACTS: concepts and technology of flexible AC transmission systems*. New York: IEEE Press; 2000.
- [15] Wang LC, Kuan BL, Prokhorov AV. Stability improvement of a two-area power system connected with an integrated onshore and offshore wind farm using a STATCOM. *IEEE Trans Ind Appl* 2017;53:867–877. [\[CrossRef\]](#)
- [16] Bakhshi MH, Rabiee A. Fuzzy based damping controller for TCSC using local measurements to enhance transient stability of power systems. *Int J Electr Power Energy Syst* 2017;85:12–21. [\[CrossRef\]](#)
- [17] Kiran SHD, Subramani C. Performance of two modified optimization techniques for power system voltage stability problems. *Alex Eng J* 2016;55:2525–2530. [\[CrossRef\]](#)
- [18] Inkollu SR, Reddy VR. Optimal setting of FACTS devices for voltage stability improvement using PSO adaptive GSA hybrid algorithm. *Eng Sci Technol Int J* 2016;19:1166–1176. [\[CrossRef\]](#)
- [19] Safari AA, Golkar MA. Controller design of STATCOM for power system stability improvement using honey bee mating optimization. *J Appl Res Technol* 2013;11:144–155. [\[CrossRef\]](#)
- [20] Yao JW, Li J, Liu R, Zhang H. Sub-synchronous resonance damping control for series-compensated DFIG-based wind farm with improved particle swarm optimization algorithm. *IEEE Trans Energy Convers* 2019;34:849–859. [\[CrossRef\]](#)
- [21] Bamba S, Gupta SK. Sub-synchronous resonance mitigation in series-compensated power systems using a GWO-based optimal controller. In: *India International Conference on Power Electronics, IICPE*. IEEE Computer Society; 2023. [\[CrossRef\]](#)
- [22] Kumar R, Singh R, Ashfaq H. Stability enhancement of multi-machine power systems using ant colony optimization-based static synchronous compensator. *Comput Electr Eng* 2020;83. [\[CrossRef\]](#)
- [23] Yousuf V, Ahmad A. Optimal design and application of fuzzy logic equipped control in STATCOM to abate SSR oscillations. *Int J Circuit Theory Appl* 2021;49:4070–4087. [\[CrossRef\]](#)
- [24] Moradi-Shahrbabak Z. Proposed sub-synchronous resonance damping controller for large-scale wind farms. *IET Renew Power Gener* 2023;17:3209–3220. [\[CrossRef\]](#)
- [25] Padiyar KR, Prabhu N. Analysis of SSR with three-level twelve-pulse VSC-based interline power-flow controller. *IEEE Trans Power Deliv* 2007;22:1688–1695. [\[CrossRef\]](#)
- [26] Farmer RG. Second benchmark model for computer simulation of subsynchronous resonance. *IEEE Power Eng Rev* 1985;PER-5:34. [\[CrossRef\]](#)
- [27] Second benchmark model for computer simulation of subsynchronous resonance. *IEEE Subsynchronous Resonance Working Group*. 1985.
- [28] Sharma PR, Gupta SK, Yadav P, Sharma PR. Optimal location of UPFC in power system using multi-objective GAPSO hybrid algorithm. *Int J Ser Eng Sci* 2016;2:26–45.
- [29] Minaxi, Saini S. Frequency control using different optimization techniques of a standalone PV-wind-diesel with BESS hybrid system. *IEEJ Trans Power Energy* 2023;143:218–225. [\[CrossRef\]](#)
- [30] Wadhwa K, Gupta SK. A novel black widow optimized controller approach for automatic generation control in modern hybrid power systems. *Int J Electr Electron Res* 2023;11:819–825. [\[CrossRef\]](#)
- [31] Wadhwa K, Gupta SK. Integrating capacitive energy storage (CES) into existing power system to manage frequency deviation. *Int J Intell Syst Appl Eng* 2024;12:737–734.

[32] Mirjalili S, Mirjalili SM, Lewis A. Grey wolf optimizer. Adv Eng Softw 2014;69:46–61. [\[CrossRef\]](#)

[33] Prasad CE, Vadhera S. Mitigation of sub synchronous resonance using STATCOM controlled by PID and FL controllers. In: 2014 IEEE 6th India International Conference on Power Electronics (IICPE). IEEE; 2014. p. 1–5. [\[CrossRef\]](#)

APPENDIX A.	
Generator data:	
Ratings: 600MVA, 22KV.	
Stability data:	
$X_1=0.14$ pu	$R_a=0.0045$ pu
$X_d=1.65$ pu	$X_q=1.59$ pu
$X'_d=0.25$ pu	$X'_q=0.46$ pu
$X''_d=0.20$ pu	$X''_d=0.20$ pu
$T'_{do}=4.5$ s	$T'_{qo}=0.67$
$T''_{do}=0.040$ s	$T''_{qo}=0.09$ s
Transmission line data: 500KV	
Line with series capacitor:	
$R_1=0.0074$ pu, $R_o=0.022$ pu, $X_1=0.08$ pu, $X_o=0.240$ pu	
Line without series capacitor:	
$R_1=0.0067$ pu, $R_o=0.0186$ pu, $X_1=0.0739$ pu, $X_o=0.210$ pu	
Transformer data;	
600MVA, 60Hz, Δ/Y , 22KV/500KV, $R_p=0.0006$ pu, $R_s=0.0006$ pu, $X_p=0$ pu, $X_s=0.12$ pu	
STATCOM parameters: 100 MVA	
System nominal voltage = 500kV, f= 60Hz,	
$R_1 = 0.00732$, $L_1 = 0.22$ H, $C=325\mu$ F	
PI Voltage Regulator gains: $K_p=5$, $K_i=1000$	